Autler-Townes effect for an atom in a 100% amplitude-modulated laser field. II. Experimental results

S. Papademetriou, M. F. Van Leeuwen, and C. R. Stroud, Jr.
The Institute of Optics, University of Rochester, Rochester, New York 14627
(Received 27 September 1994; revised manuscript received 12 October 1995)

We report the observation of the Autler-Townes absorption spectrum of a two-level atom in a 100% amplitude-modulated optical field. Two frequency-stabilized dye lasers interact with a three-level atomic cascade system. One of the two lasers is used to create the bichromatic field that saturates the lower transition, while the second one is tuned in the frequency between the second and third levels to probe the absorption line shape. We investigate the dependence of the spectrum on the detuning between the average frequency of the bichromatic field and the lower atomic resonance. In order to study the effects of saturation, for every value of the detuning we take a series of data for different intensity levels of the bichromatic field. There is very good agreement between theory and experiment and profound differences from the conventional Autler-Townes results with a monochromatic pump field.

PACS number(s): 42.50.Hz, 32.80.−t

I. INTRODUCTION

The interaction of a two-level atomic system with a strong monochromatic field has been the subject of a great deal of theoretical and experimental study [1]. The detailed understanding of this interaction, and especially its fluorescence spectrum, has been an important achievement of quantum optics [2,3].

One interesting generalization of these studies is resonant interactions with finite bandwidth laser fields [4]. Another obvious and intriguing generalization is that of a strong 100% amplitude-modulated (AM) field with a two-level atom. It is more than an interesting academic generalization, since the interaction of a strong bichromatic field with a two-level atomic system is fundamental to a number of research disciplines, including nonlinear optics [5–25] and laser theory [26–30].

More recently, there has been much interest, both experimental [31] and theoretical [32,33], in the resonance fluorescence spectrum of an atom subject to bichromatic excitation. Zhu *et al.* [31] have experimentally demonstrated how this spectrum differs qualitatively from the characteristic triplet spectrum of an atom excited by a strong monochromatic field. They found that the resonance fluorescence spectrum of a strong bichromatic field, with its average frequency on resonance with a two-level atom, consists of a number of symmetric sidebands separated by half of the frequency difference between the two strong fields (i.e., the modulation frequency δ). Furthermore, it is evident from their data (Fig. 2 of Zhu *et al.* [31]) that the odd sidebands are narrower than the even ones. The elastic parts of the spectrum, which are relatively narrow and occur only at odd multiples of the sideband separation, contribute to this variation in widths. For increased intensities the contribution of inelastically scattered light predominates over the elastically scattered and hence should be responsible for observable variations in the widths of the spectral components in this regime.

In this paper we show the results of an experimental study of the probe absorption spectrum of an atomic resonance driven by an AM field. The AM field interacts with the lower two levels of a three-level cascade system, while a weak probe is tuned in frequency near the transition frequency between the upper two levels. We monitor the absorption of the weak probe as a function of its detuning for different intensity levels of the AM field. We also study the effects that detuning between the average frequency of the AM field and the lower atomic resonance has on the absorption spectrum of the weak probe. This regime has not been examined to date, to our knowledge.

Our setup is the bichromatic equivalent of the Autler-Townes experiment [34]. The overall structure of the absorption spectrum is very similar to that of the resonance fluorescence emission spectrum [31]. When the average frequency of the AM field is on resonance with the lower transition, we find that all peaks separated from the atomic resonance by even multiples of the modulation frequency have the same width. Similarly, all peaks separated from resonance by odd multiples of the modulation frequency have the same width. The actual width of an even or odd peak depends upon the ratio of the Rabi frequency to the modulation frequency of the bichromatic field as well as on the natural widths of the atomic states [35,36]. Whether the odd or even peaks are wider depends on this ratio.

In Sec. II we give a detailed explanation of the experimental setup and the procedure used to obtain our data. In Sec. III we describe numerical modeling of the experiment. In the preceding paper [36] we have presented analytic solutions for the absorption spectrum of the weak probe in our setup, when the bichromatic field is on resonance with the lower transition. In Secs. IV and V we give an analysis of our results and a conclusion.

II. EXPERIMENTAL APPARATUS AND PROCEDURE

Our experiment is performed using a collimated sodium atomic beam prepared by optical pumping in the $3\,^2S_{1/2}(F=2,m_F=2)$ sublevel of the ground state [21,37]. Details of the atomic beam are given in Refs. [20,38]. Levels $|a\rangle$, $|b\rangle$ and $|c\rangle$ in Fig. 1(a) correspond to the $3\,^2S_{1/2}(F=2,m_F=2)$, $3^2P_{3/2}(F=3,m_F=3)$, and

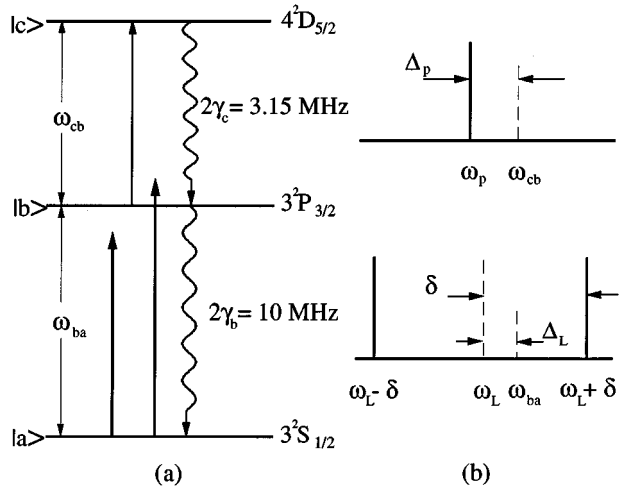

FIG. 1. (a) Energy-level diagram of Na, showing the three levels involved in the interaction under study. The spontaneous decay rates out of $|b\rangle$ and $|c\rangle$ are γ_b and γ_c, respectively. Laser 1 is the AM field interacting with the lower transition. Laser 2 is the weak monochromatic tunable probe interacting with the upper two levels. (b) Frequency notations: the average frequency of the bichromatic field is ω_L; the modulation frequency δ is defined as half the frequency separation of the two fields in the lower transition; the detuning of the pump laser is defined as $\Delta_L \equiv \omega_L - \omega_{ba}$, where ω_{ba} is the frequency separation between $|b\rangle$ and $|a\rangle$; the detuning of the monochromatic weak probe is $\Delta_p \equiv \omega_p - \omega_{cb}$, where ω_p is the frequency of the laser field in the upper transition and ω_{cb} is the frequency separation between $|c\rangle$ and $|b\rangle$.

$4^2D_{5/2}(F=4, m_F=4)$ sublevels, respectively. The spontaneous decay rates of the two excited state levels are $2\gamma_b/(2\pi)=10$ MHz and $2\gamma_c/(2\pi)=3.15$ MHz [39,40]. Since in our experiment all transitions are purely radiatively broadened, γ_b and γ_c are also equal to half the linewidths of the corresponding atomic levels. In deference to previously established conventions [20,21] we have used T_2^{-1} to describe the decay rates in our system. The reader should note that this differs from the convention of our theoretical analysis such that γ_b and γ_c are equivalent to $\Gamma_b/2$ and $\Gamma_c/2$, respectively, of Ref. [36].

The strong bichromatic field and the beam used for optical pumping are derived from laser 1 (Fig. 2). They both interact with the $|a\rangle \leftrightarrow |b\rangle$ transition near 5890 Å, the D_2 line of sodium. The overall linewidth of this actively stabilized laser is less than 1 MHz [20,21]. The AM optical field is created with the help of an 80-MHz acousto-optic modulator (A-O 1). The 0 and -1 orders of A-O 1 are combined with a 50%-50% beam splitter and high reflector. The resulting bichromatic field is monitored with a fast photodiode (rise time $\tau_r \leqslant 1$ nsec) and oscilloscope in order to ensure that the heterodyne signal is fully amplitude modulated [21]. With a modulation frequency of 40 MHz there are will be, on average, four modulation periods within the lifetime of the atomic level $|b\rangle$.

Laser 2 (Fig. 2) is a ring dye laser, frequency stabilized in a manner similar to that of laser 1, with a residual linewidth of less than 1 MHz. We use rhodamine 6G in both dye lasers. Laser 2 operates at 5688 Å and interacts with the $|b\rangle \leftrightarrow |c\rangle$ transition in Fig. 1(a).

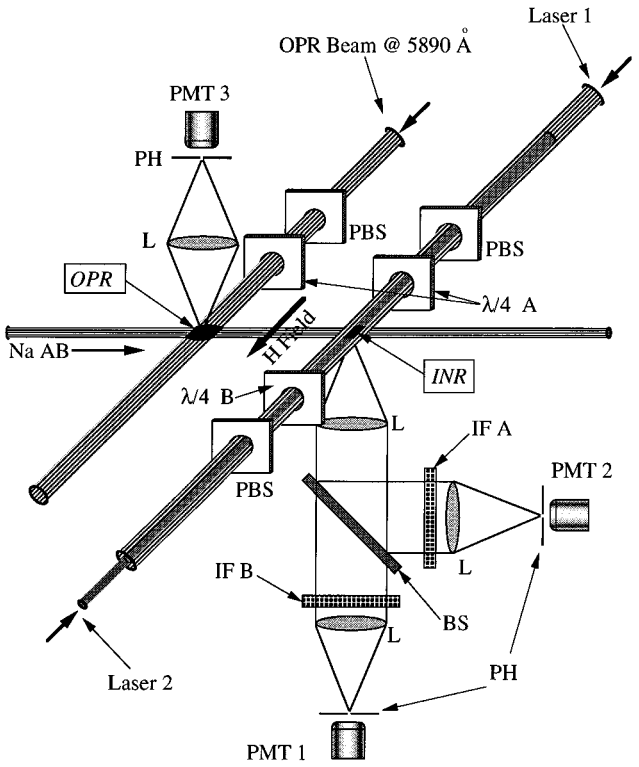

FIG. 2. Atomic beam setup. The following labeling conventions are used in this figure: Na AB, sodium atomic beam; PMT, photomultiplier tube; BS, 50%-50% beam splitter; IF A, interference filter at 5890 Å; IF B, interference filter at 5688 Å; L, 100-mm planoconvex lens; λ/4 A, zeroth-order quarter-wave plate at 5890 Å; λ/4 B, zeroth-order quarter-wave plate at 5688 Å; PBS, polarizing beam splitter; OPR, optical pumping region; INR, interaction region; PH, 0.5-mm pinhole; H field, magnetic field.

The light intensity of the probe field, laser 2, is attenuated by passing it through another acousto-optic modulator (A-O 2) and using its first diffracted order. Its intensity is measured at the interaction region with a powermeter and throughout the experiment is maintained at the same constant level of 550 μW/cm^2. The saturation intensity of the $|b\rangle \leftrightarrow |c\rangle$ transition is 750 μW/cm^2. It is necessary to keep laser 2 below the saturation intensity of the upper transition in order to prevent any excess power broadening contributions from that laser. The probe laser is varied in frequency while remaining stabilized. Its detuning is defined as $\Delta_p \equiv \omega_p - \omega_{cb}$ [see Fig. 1(b)], where ω_p is the frequency of the probe laser and ω_{cb} is the frequency of the atomic transition between levels $|c\rangle$ and $|b\rangle$.

One of the most important aspects of the experimental setup is the fact that we always use a secondary beam on resonance with the lower transition to perform the optical pumping. Prior to creating the bichromatic field we split off a portion of the monochromatic beam with which we monitor the value of the center frequency of the modulated field and perform the optical pumping. This, along with the application of a magnetic field of 1 G in the direction of propagation of the bichromatic field (Fig. 2), proves to be sufficient for maintaining a good quality three-level atomic system [37,41].

Before the light fields interact with the atomic beam they

are expanded and collimated. The beam that performs the optical pumping has a diameter of 2 mm and intercepts the atomic beam 6 mm downstream from the interaction region (see Fig. 2). The choice of the beam size of the optical pumping beam and its distance from the interaction region is made by spectrosopically monitoring how well the optical pumping is maintained [41]. The probe and bichromatic fields are also collimated and expanded to a 3 mm diameter at the interaction region. The reason for expanding the laser fields before entering the interaction region is to ensure that when the photomultiplier tube (PMT 1 in Fig. 2) that monitors the upper transition detects a signal, it is from the center of the Gaussian beam profiles of the two beams. In this way we minimize transverse intensity variations within the region from which we obtain our signal. The two beams interacting with the three-level atoms are collinear but counterpropagating so that much of the residual Doppler broadening is canceled [39,40].

In order to vary the Rabi frequency of the pump laser in the lower transition, we use a variable neutral density filter before we send the bichromatic field to the atomic beam. This way we can investigate the effects that the Rabi frequency of the AM field has on the absorption spectrum of the weak probe in the upper transition.

The pump, probe, and optical pumping beams interact with the atomic beam as shown in Fig. 2. Each of the three beams goes through a polarizing beam splitter and quarter-wave plate. The beam splitters have extinction ratios of 10^4:1 and the wave plates are zeroth order. This, along with careful alignment of their optic axes, ensures a good circular polarization state for all three laser beams. Fine tuning of the polarization state of all three beams is done spectroscopically by ensuring that only the appropriate Zeeman sublevels are involved in the interaction [41].

The interaction region where the two laser beams and the atomic beam intersect is imaged through a beam splitter and interference filters onto two pinholes. The beam splitter and the filters allow the fluorescence from the two transitions to be monitored separately. The pinholes allow the photomultipliers to collect light from only the central 0.5-mm of the interaction region where the laser intensities are approximately constant. The optical pumping region is monitored with PMT 3 through a 0.5 mm pinhole. The signal from PMT 3 is always maintained at a maximum to ensure proper optical pumping. All three PMT's used have a quantum efficiency of 10% at 600 nm.

III. NUMERICAL MODELING

We have modeled the experiment with the stationary solutions of the density-matrix equations of motion obtained numerically with the use of Floquet's theorem [10,21,29]. The time-averaged fluorescent intensity scattered from the upper transition is the quantity we measure in our experiment. This is proportional to the population of level $|c\rangle$ [Fig. 1(a)]. In all the theoretical fits shown here, we plot the time-averaged population of level $|c\rangle$, with solid lines [42]. All relevant frequencies in this work are normalized to the half-width at half maximum (HWHM) of level $|b\rangle$, $\gamma_b = 1/T_b$ [see Fig. 1(a)]. For sodium, $T_b = 33$ nsec. All theoretical plots shown are convolved with a Gaussian with a full width at half maximum (FWHM) of 10 MHz. This convolution seems to best simulate all the averaging mechanisms present in our experiment but not included in this theory, as described later in Sec. IV.

While the Floquet treatment of the dynamics gives good agreement with the experimental results, it does not provide us with any physical intuition to the complicated dynamics. In the preceding paper, Van Leeuwen *et al.* [36], using a dressed-state analysis of the atom-field interaction, have derived analytic expressions for both the absorption spectrum of the probe in the upper transition, as well as the linewidths of the different sidebands, when the center frequency of the intense AM field is on resonance with the lower transition. In this paper we will restrict ourselves to the numerical results in the analysis of our measured spectra.

IV. EXPERIMENTAL RESULTS

The data are taken by the x and y channels of a transient digitizer. The x channel is driven by an external ramp signal from laser 2, the probe laser, which is synchronized with the sweep voltage that tunes it. The y channel is the output of PMT 1 (see Fig. 2) after it goes through a current to voltage converter. PMT 1 monitors the total scattered fluorescent intensity from the upper transition $|b\rangle \leftrightarrow |c\rangle$ as a function of detuning Δ_p of the probe laser.

The tuning range of the data is chosen so that it covers all the detectable structure of the absorption spectrum for the maximum Rabi frequency used in each detuning case. The frequency difference between the two fields in the lower transition is twice the modulation frequency 2δ [see Fig. 1(b)]. This is the rf carrier frequency of A-O 1. All our data are taken with $2\delta = 80$ MHz. To improve the signal-to-noise ratio, we take the average of eight frequency sweeps of the probe laser. In every plot, we show the experimental results along with the best theoretical fit. The scaling of the frequency axis is performed with the aid of the smallest Rabi frequency data set. For a weak bichromatic field in the lower transition, the absorption spectrum should be two Lorentzians separated by the frequency difference of the two fields. In our setup, for example, the two peaks in Fig. 3(a) are separated by 80 MHz. This scaling is used for all the experimental plots shown in this paper.

We used only two parameters for fitting the experimental results: the Rabi frequency of the components of the AM field and an overall amplitude scale factor. In order to get the best fit to the data we convolve the results of the theoretical calculations with a Gaussian with a FWHM of 10 MHz. This convolution simulates the averaging mechanisms present in the experiment but not included in the equations of the density-matrix elements. These averaging mechanisms include intensity averaging due to nonuniformities of the Gaussian laser beam profiles and detuning averaging due to the fact that the laser beams are not perfect plane waves at the interaction region. Although the Rabi frequency of the AM field was used as a free parameter, the resultant value from the fitting process was within 5% of the value measured during the experiment. The small discrepancy is attributed solely to inacuracies of the measurement of the beam waist at the interaction region [35]. The value for the Rabi frequency of the weak monochromatic field in the upper transition is set

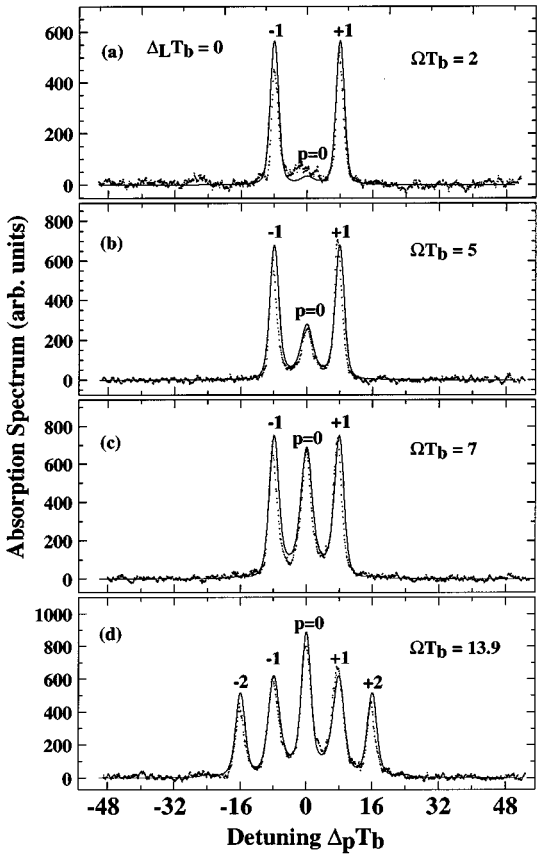

FIG. 3. Time-averaged scattered fluorescent intensity from the $|b\rangle \leftrightarrow |c\rangle$ transition as a function of detuning of the probe laser. The experimental data are shown by dots, whereas the best theoretical fit is shown by a solid line. The average frequency of the bichromatic field in the lower transition is on resonance with the $|a\rangle \leftrightarrow |b\rangle$ transition $\Delta_L T_b = 0$. The Rabi frequency for the components of the bichromatic field are derived from the best theoretical fit to each of the data plots. (a)–(d) correspond to Rabi frequencies of $\Omega T_b = 2,5,7,13.9,$ respectively.

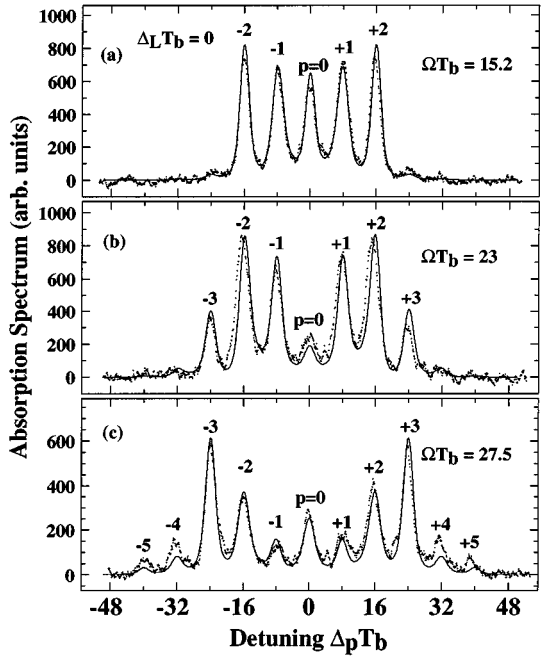

FIG. 4. Time-averaged scattered fluorescent intensity from the $|b\rangle \leftrightarrow |c\rangle$ transition as a function of detuning of the probe laser. The experimental data are shown by dots, whereas the best theoretical fit is shown by a solid line. The average frequency of the bichromatic field in the lower transition is on resonance with the $|a\rangle \leftrightarrow |b\rangle$ transition $\Delta_L T_b = 0$. The Rabi frequency for the components of the bichromatic field are derived from the best theoretical fit to each of the data plots. (a)–(c) correspond to Rabi frequencies of $\Omega T_b = 15.2, 23, 27.5,$ respectively.

equal to $0.185 T_b$, which corresponds to an intensity of 550 μW/cm^2.

The resonant case ($\Delta_L T = 0$) is depicted in Figs. 3 and 4. We start from a low value of the Rabi frequency of each of the components of the bichromatic field [$\Omega T_b = 2$ in Fig. 3(a)] and went up to the highest value attainable by our setup [$\Omega T_b = 27.5$ in Fig. 4(c)]. The numbering on the peaks corresponds to that suggested in Sec. V of Van Leeuwen *et al.* [36]. This way we can identify each peak with the corresponding transitions involved in the dressed-state picture of the system.

For the resonant case, there are several important points to be outlined. In contrast to the well-studied case of a monochromatic field in the lower transition [34,39,40], the position of the peaks of the absorption spectrum are independent of the Rabi frequency. As we increase the Rabi frequency and power broaden the lower transition more peaks emerge, spaced at frequency intervals of the modulation frequency δ. The relative amplitudes and widths of these peaks depend on the ratio of the Rabi frequency to the modulation frequency [31–33,36].

In Fig. 5 we show the effects that the Rabi frequency has on the widths of the different order peaks of the absorption spectrum. The variation of the normalized widths γT_b of the different peaks of the absorption spectrum as a function of the Rabi frequency is shown. As in Eq. (5.6) of Van Leeuwen *et al.* [36], the widths of the individual peaks depend on the ratio of the Rabi frequency to the modulation frequency. To

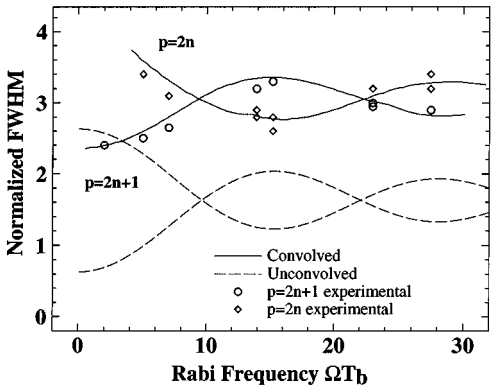

FIG. 5. Normalized FWHM of the even and odd peaks of the absorption spectrum as a function of the Rabi frequency ΩT_b. The average frequency of the bichromatic field is on resonance with the lower atomic transition $\Delta_L T_b = 0$. The modulation frequency is held constant at $\delta T_b = 8$. The dashed lines are the theoretical predictions $2\gamma_p T_b = 2\gamma_c T_b + \gamma_b T_b[1 + (-1)^p J_0(2\Omega/\delta)]$ (Eq. 4.3 of Ref. [38]). The solid lines are the theoretical predictions after a convolution with a Gaussian of FWHM equal to 10 MHz. The FWHM of the even orders ($p = 2n$) and odd orders ($p = 2n+1$) from the experimental plots are also shown, with $n = 0,1,2, \ldots$.

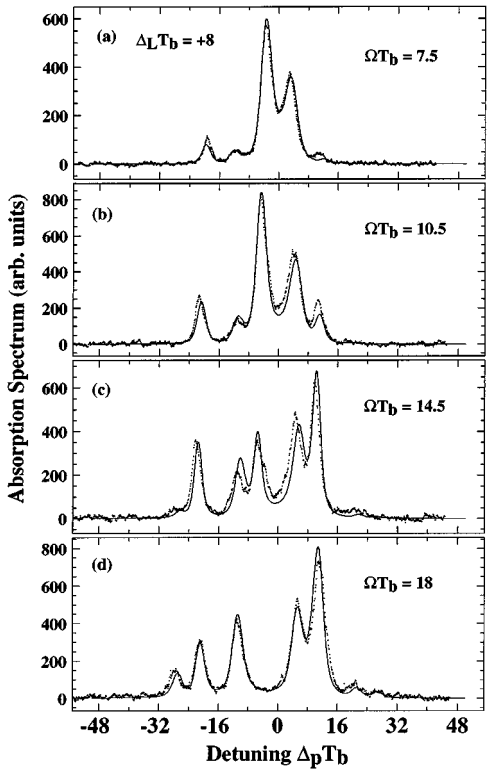

FIG. 6. Time-averaged scattered fluorescent intensity from the $|b\rangle \leftrightarrow |c\rangle$ transition as a function of detuning of the probe laser. The experimental data are shown by dots, whereas the best theoretical fit is shown by a solid line. The average frequency of the bichromatic field in the lower transition is blueshifted by 40 MHz from the $|a\rangle \leftrightarrow |b\rangle$ transition $\Delta_L T_b = 8$. The Rabi frequency for the components of the bichromatic field are derived from the best theoretical fit to each of the data plots. (a)–(d) correspond to Rabi frequencies of $\Omega T_b = 7.5, 10.5, 14.5, 18$, respectively.

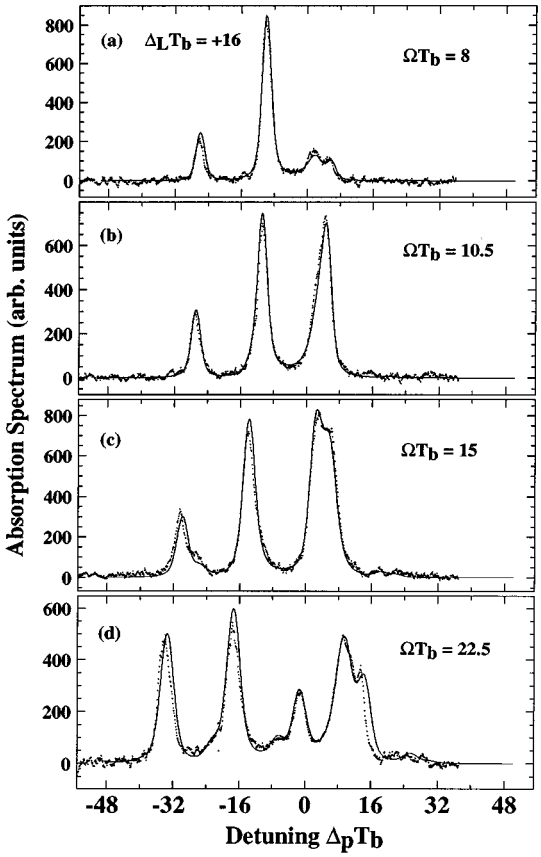

FIG. 7. Time-averaged scattered fluorescent intensity from the $|b\rangle \leftrightarrow |c\rangle$ transition as a function of detuning of the probe laser. The experimental data are shown by dots, whereas the best theoretical fit is shown by a solid line. The average frequency of the bichromatic field in the lower transition is blueshifted by 80 MHz from the $|a\rangle \leftrightarrow |b\rangle$ transition $\Delta_L T_b = 16$. The Rabi frequency for the components of the bichromatic field are derived from the best theoretical fit to each of the data plots. (a)–(d) correspond to Rabi frequencies of $\Omega T_b = 8, 10.5, 15, 22.5$, respectively.

best simulate our experiment, where the modulation frequency remains fixed, we plot the FWHM of the even and odd ordered peaks of the absorption spectrum, as a function of the Rabi frequency, while the modulation frequency remains constant $\delta T_b = 8$.

It is evident from Fig. 5 that the widths of the peaks change as we vary the Rabi frequency. For a given Rabi frequency, all even (odd) peaks have the same width. Depending on the value of the Rabi frequency, the even peaks can be wider than the odd ones or vice versa. The experimental values are in good agreement with the theoretical predictions.

The absorption spectra we have measured correspond to a direct probe of a two-level resonance strongly driven by a resonant AM field. The widths of the peaks, in the limit in which they can be resolved (i.e., $\delta \gg \gamma_b$), provide the widths of the levels of the resonantly dressed atom without the complication of the Rayleigh spectrum that is present in the resonance fluorescence spectrum. They therefore provide information from which the widths of the components of the inelastically scattered fluorescence spectrum can be inferred.

We have also looked at the effects that the detuning Δ_L of the bichromatic field has on the absorption spectrum. We investigated three different values of detuning. The case where $\Delta_L T = 8$ is depicted in Fig. 6. We show a series of plots for the time-averaged absorption spectrum of the weak probe. In Fig. 7 we show another set of data for the absorption spectrum for $\Delta_L T = 16$. Note that for the cases of Figs. 6 and 7, the spectrum becomes asymmetric about the zero position ($\Delta_p T = 0$). Also the position of the peaks changes as the Rabi frequency is varied.

Finally, in Fig. 8 we show a representative case for a redshifted detuning $\Delta_L T = -8$. We chose a value for the Rabi frequency that is as close as possible to an equivalent blueshifted case [Fig. 6(c)]. In Fig. 8, $\Omega T_b = 15$. Note that the resultant absorption spectrum is a mirror image, about the zero value of the probe detuning, of the equivalent blueshifted Rabi frequency [i.e., Fig. 6(c) and 8] due to energy conservation of the probe photons.

V. CONCLUSION

We have presented an experimental study of the time-averaged absorption spectrum for a weak laser field probing the upper transition of a three-level atomic cascade, the lower transition of which is quasiresonantly driven by a bichromatic field. We have studied the effects that both the Rabi frequency and detuning of the bichromatic field in the

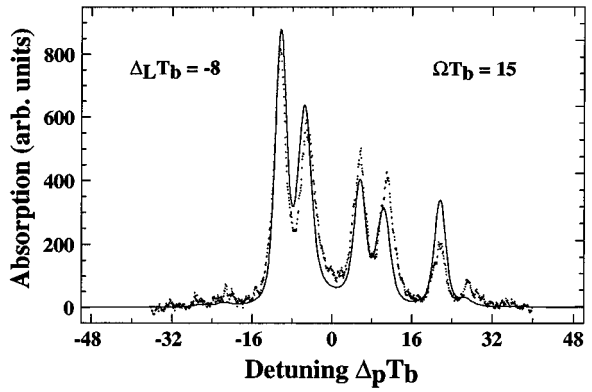

FIG. 8. Time-averaged scattered fluorescent intensity from the $|b\rangle \leftrightarrow |c\rangle$ transition as a function of detuning of the probe laser. The experimental data are shown by dots, whereas the best theoretical fit is shown by a solid line. The average frequency of the bichromatic field in the lower transition is redshifted by 40 MHz from the $|a\rangle \leftrightarrow |b\rangle$ transition, $\Delta_L T_b = -8$. The Rabi frequency for the components of the bichromatic field is derived from the best theoretical fit to the data. $\Omega T_b = 15$.

lower transition have on the absorption spectrum of the weak probe in the upper transition.

For the resonant case $\Delta_L T = 0$ we find that the position of the peaks of the absorption spectrum are separated by the modulation frequency, independent of the Rabi frequency. Also, the absorption spectrum is symmetric about the zero value of the detuning of the probe field. As the Rabi frequency of the bichromatic field is increased the spectrum broadens as more higher-order peaks begin emerging. The dressed-state analysis [36] provides an intuitive picture of transitions between the bare and dressed states of a bichromatically driven system.

Three different detuning values of the center frequency of the bichromatic field were also investigated. The absorption spectrum ceases to be symmetric about the zero value of the probe field detuning. As the Rabi frequency is increased more peaks start emerging but, in contrast to the on-resonance case, their positions do not remain fixed. The spectrum now consists of pairs of peaks separated by twice the modulation frequency, independent of the pump detuning and Rabi frequency. The absolute position and splitting of a pair of resonances vary as a function of the detuning and Rabi frequency of the pump. This again can be interpretted in the dressed-state picture [43] with a detuned bichromatic field.

Finally, we believe that, with this experiment, we have unambiguously established that the widths of neighboring peaks in the Autler-Townes absorption spectrum for a two-level atom in a bichromatic field alternate between narrow and broad as a function of the Rabi frequency Ω, as seen also in the resonance fluorescence spectrum from this system [31]. This result is consistent with a dressed-state analysis [32], which predicts a dependence of the widths upon the ratio the Rabi frequency to the modulation frequency Ω/δ [see Eq. (5.6) of Van Leeuwen *et al.* [36]].

ACKNOWLEDGMENT

This work was supported by the Army Research Office.

[1] P. L. Knight and P. W. Milonni, Phys. Rep. **66**, 21 (1980).
[2] B. R. Mollow, Phys. Rev. **188**, 1969 (1969).
[3] F. Schuda, C. R. Stroud, Jr., and M. Hercher, J. Phys. B **7**, L198 (1974).
[4] D. S. Elliott and S. J. Smith, J. Opt. Soc. Am. B **5**, 1927 (1988).
[5] A. M. Bonch-Bruevich, T. A. Vartanyan, and N. A. Chigir, Zh. Éksp. Teor. Fiz. **77**, 1899 (1979) [Sov. Phys. JETP **50**, 901 (1979)].
[6] S. P. Goreslavsky and V. P. Krainov, Zh. Éksp. Teor. Fiz. **76**, 26 (1979) [Sov. Phys. JETP **49**, 13 (1979)].
[7] G. I. Toptygina and E. E. Fradkin, Zh. Éksp. Teor. Fiz. **82**, 429 (1982).
[8] V. Hizhnyakov and M. Rozman, Opt. Commun. **52**, 183 (1984).
[9] A. A. Mak, S. G. Przhibel'skii, and N. A. Chigir, Izv. Akad. Nauk. SSSR, Ser. Fiz. **47**, 1976 (1983).
[10] G. S. Agarwal and N. Nayak, J. Opt. Soc. Am. B **1**, 164 (1984).
[11] G. S. Agarwal and N. Nayak, Phys. Rev. A **33**, 391 (1986).
[12] J. H. Eberly and V. D. Popov, Phys. Rev. A **37**, 2012 (1988).
[13] T. W. Mossberg and M. Lewenstein, Phys. Rev. A **39**, 163 (1989).
[14] P. Thomann, J. Phys. B **13**, 1111 (1980).
[15] B. Blind, P. R. Fontana, and P. Thomann, J. Phys. B **13**, 2717 (1980).
[16] S. P. Tewari and M. K. Kumari, J. Phys. B **22**, L475 (1989).
[17] R. E. Silverans, G. Borghs, P. D. Bisschop, and M. van Hove, Phys. Rev. Lett. **55**, 1070 (1985).
[18] N. Tsukada, Phys. Rev. A **39**, 5797 (1989).
[19] S. P. Tewari and M. K. Kumari, Phys. Rev. A **41**, 5273 (1990).
[20] S. Chakmakjian, K. Koch, and C. R. Stroud, Jr., J. Opt. Soc. Am. B **5**, 2015 (1988).
[21] S. Papademetriou, S. Chakmakjian, and C. R. Stroud, Jr., J. Opt. Soc. Am. B **9**, 1182 (1992).
[22] M. A. Newbold and G. J. Salamo, Phys. Rev. A **22**, 2098 (1980).
[23] W. M. Ruyten, J. Opt. Soc. Am. B **6**, 1796 (1989).
[24] W. M. Ruyten, Phys. Rev. A **40**, 1447 (1989).
[25] Qilin Wu, Daniel J. Gauthier, and T. W. Mossberg, Phys. Rev. A **49**, R1519 (1994).
[26] B. J. Feldman and M. S. Feld, Phys. Rev. A **1**, 1375 (1970).
[27] L. W. Hillman, J. Krasinski, R. W. Boyd, and C. R. Stroud, Jr., Phys. Rev. Lett. **52**, 1605 (1985).
[28] L. W. Hillman, J. Krasinski, K. Koch, and C. R. Stroud, Jr., J. Opt. Soc. Am. B **2**, 211 (1985).
[29] K. Koch, B. J. Oliver, S. H. Chakmakjian, and C. R. Stroud, Jr., J. Opt. Soc. Am. B **6**, 58 (1989).
[30] C. R. Stroud, Jr., K. Koch, and S. Chakmakjian, in *Proceedings of the International Conference on Optical Instabilities, Rochester, 1986*, edited by R. W. Boyd, M. G. Raymer, and L. M. Narducci (Cambridge University Press, Cambridge, 1986).

[31] Y. Zhu, A. Lezama, D. J. Gauthier, and T. Mossberg, Phys. Rev. A **41**, 6574 (1990).
[32] H. S. Freedhoff and Z. Chen, Phys. Rev. A **41**, 6013 (1990); **46**, 7328(E) (1992).
[33] G. S. Agarwal, Y. Zhu, D. J. Gauthier, and T. Mossberg, J. Opt. Soc. Am. B **8**, 1163 (1991).
[34] S. H. Autler and C. H. Townes, Phys. Rev. **100**, 703 (1955).
[35] S. Papademetriou, Ph.D. thesis, University of Rochester, 1993 (unpublished).
[36] M. F. Van Leeuwen, S. Papademetriou, and C. R. Stroud, Jr., preceding paper, Phys. Rev. A **53**, 990 (1996).
[37] J. A. Abate, Opt. Commun. **25**, 359 (1978).
[38] S. Chakmakjian, Ph.D. thesis, University of Rochester, 1990 (unpublished).
[39] H. R. Gray and C. R. Stroud, Jr., Opt. Commun. **25**, 359 (1978).
[40] P. R. Hemmer, B. W. Peuse, F. Y. Wu, J. E. Thomas, and S. Ezekiel, Opt. Lett. **6**, 531 (1981).
[41] M. L. Citron, H. R. Gray, C. W. Gabel, and C. R. Stroud, Jr., Phys. Rev. A **16**, 1507 (1977).
[42] In Ref. [21] we show how the time-averaged population of level $|c\rangle$ is proportional to the absorption of the field in the upper transition, which is the quantity we are really measuring.
[43] Z. Ficek and H. S. Freedhoff, Phys. Rev. A **48**, 3092 (1993).